ELSEVIER

Journal of Nuclear Materials 313–316 (2003) 1287–1291

journal of nuclear materials

www.elsevier.com/locate/jnucmat

# Influence of magnetic field configurations on divertor plasma parameters in the W7-AS stellarator

P. Grigull *, K. McCormick, Y. Feng, A. Werner, R. Brakel, H. Ehmler, F. Gadelmeier, D. Hartmann, D. Hildebrandt, R. Jaenicke, J. Kisslinger, T. Klinger, R. König, D. Naujoks, H. Niedermeyer, N. Ramasubramanian, F. Sardei, F. Wagner, U. Wenzel, The W7-AS Team

*Max-Planck-Institut für Plasmaphysik, EURATOM Ass., Boltzmannstrasse 2, D-85748 Garching, Germany*

Received 27 May 2002; accepted 12 September 2002

**Abstract**

The new island divertor in W7-AS enables quasi steady-state operation with NBI at very high density including scenarios with stable detachment from the targets. Experiments with reversed $B$-field indicate that the interaction zones on the targets are affected in first order by $E \times B$ drifts. Stable detachment is restricted to magnetic field configurations with sufficiently large separation between $x$-points and targets and not too small field line pitch inside the islands. It is always partial in the sense that it does not extend over the full target area. This inhomogeneity is ascribed to an in/out asymmetry of the electron temperature at the upstream separatrix position.


*PACS:* 52.40.H
*Keywords:* Boundary plasma; Stellarators; Divertor

## 1. Introduction

The W7-AS stellarator is presently being operated with an island divertor in order to experimentally evaluate this plasma exhaust concept in view of future application to W7-X. The divertor enables access to a new, promising operating regime with NBI at very high density with significantly improved energy and drastically reduced impurity confinement (High Density H-mode, HDH [1–4]). These features allow quasi steady-state operation also under conditions of partial detachment from the divertor targets. Whereas the HDH regime has been proven as rather robust against variations of the magnetic field configuration within a broad range, the near-target plasma and the energy and particle deposition zones in this 3D geometry show a varying, multifarious picture, and stable partial detachment is restricted to specific configurations. The present study is focused on this latter issue and describes details of the deposition zone phenomenology on the targets in relation to core parameters and the vacuum magnetic field topology.

## 2. Magnetic field configuration and divertor geometry of W7-AS

W7-AS ($R = 2$ m, $a \leqslant 0.16$ m, $B \leqslant 2.5$ T) is a modular, low-shear stellarator with five magnetic field periods. Depending on the adjustable rotational transform, the plasma is bounded either by smooth flux surfaces or by a separatrix formed from naturally occurring magnetic islands at values of the edge rotational transform $\iota_a = 5/m$ $(m = 8, 9, 10, \ldots)$. The radial position of the islands can be adjusted by fine-tuning of $\iota$; their radial

* Corresponding author. Tel.: +49-089 3299 1619; fax: +49-89 3299 2584.
*E-mail address:* grigull@ipp.mpg.de (P. Grigull).

0022-3115/03/$ - see front matter 
PII: S0022-3115(02)01499-X

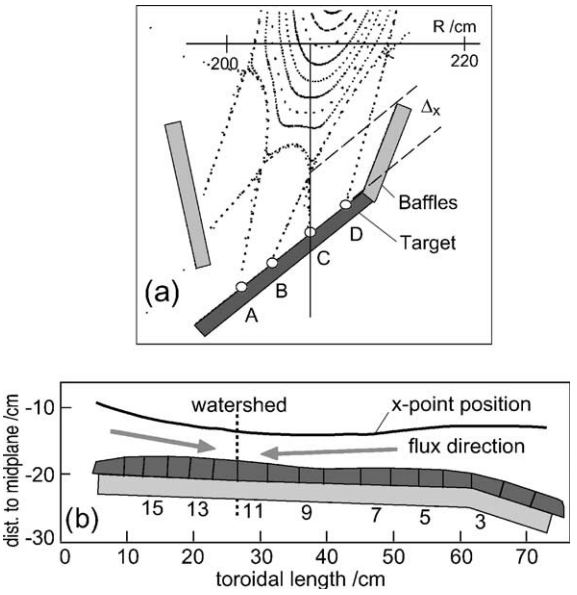


Fig. 1. (a) Cross-section of a bottom divertor module and Poincare plot of a vacuum magnetic field configuration at $\iota_a = 5/9$. Letters A–D denote intersections of the island separatrix ('island fans', see text) with the target. $\Delta_x$ indicates the minimum separation between $x$-points and target. (b) Helical cross-section of a target along the thin vertical line indicated in (a), and $x$-point vertical positions. Numbers denote target tiles as used in the text.

extent can be varied by currents $I_{cc}$ through special control coils affecting the $B_{5,m}$ perturbation field magnitude. The divertor is optimized for 5/9 boundary islands. It consists of ten identical modules – two per field period – symmetrically arranged at the top and bottom of the elliptical cross-sections. Each module is composed of an inertially cooled target (CFC) which intersects the islands (Fig. 1), and of baffles (isotropic graphite). The targets are three-dimensionally shaped. Most target tiles are instrumented with thermocouples; two opposite (top and bottom) modules are equipped with target-integrated, flush-mounted Langmuir probe arrays (tiles 5 and 13). The field line connection lengths $L_c$ from the targets to upstream as well as the distances $\Delta_x$ between $x$-points and targets – both being relevant for the divertor performance – can be independently varied within a rather large range (for details see Ref. [1]).

## 3. Strike lines and interaction zone phenomenology

In W7-AS configurations with $\iota_a = 5/9$, a boundary magnetic island which closes after 9/5 toroidal turns is twice intersected by each of the ten targets, Fig. 1. Since the deposition patterns on the targets are two-dimensional in this geometry, Fig. 1 introduces tile numbers as a toroidal coordinate. The target tile closest to the main plasma separatrix (tile 12, 'watershed') separates clockwise from counter-clockwise streaming particle and energy flows onto the target. From field line diffusion simulation follows that tiles 1–11 should be intersected by flows along the island fans B and D, tiles 12–17 by the flow along fan C. Corresponding complementary fans should be mutually shadowed by other target modules; flows along fan A as well as flows towards the baffles are completely shadowed. As Fig. 2 demonstrates e.g. for NBI discharges ($H^0 \rightarrow H^+$, absorbed power $P_{NBI}^{abs} = 1.4$ MW) in the so called standard divertor configuration (SDC, $\iota_a = 5/9$, $I_{cc} = 3.5$ kA, $B = -2.5$ T, vertical field $B_v = -100$ G), measured interaction patterns significantly deviate from these simple, geometrical expectations. The figure shows ion saturation current $I_s$ poloidal profiles measured by the Langmuir probe arrays at tile13 (top and bottom) for positive and negative $B$-field direction and three different values of the line-averaged density which characterize the development from attached to partially detached scenarios in the HDH regime. In agreement with $H_\alpha$ data, the profiles show strong peaks at positions which should be shadowed (tiles 13), and a top/bottom asymmetric shift of the peak positions and development of the peak intensities towards detachment which nearly invert with $B$-field reversal. Peaks of the downstream temperature $T_{ed}$ correspond to the $I_s$ peaks and behave analogously. A clear dependence of the ion mass ($D^0 \rightarrow D^+$ injection) was not observed. All together, these are strong indications for $E \times B$ drift effects. Corresponding $E$-fields have not yet been experimentally identified, but first simulations by the EMC3–EIRENE edge transport code – with the $E$-field being derived from the sheath potential and thermo-currents flowing along field lines between targets – could qualitatively reproduce the tendencies obtained at $B$-field reversal [5].

## 4. Partial detachment

Above a certain threshold line-averaged density $\bar{n}_e$, which increases with heating power [2], the plasma detaches from target tiles 7–17. The power flux (from thermography) becomes reduced by about a factor of ten. The $H_\alpha$ intensity is decreased by nearly the same factor indicating strongly reduced particle fluxes, and then increases towards the highest densities (lowest downstream temperatures) [2,3]. The reduction of the particle flux is consistent with nearly vanishing $I_s$ values from probes (e.g. Fig. 2, tile 13). In contrast, thermal and particle fluxes onto tiles 1–6 are much less reduced. Fig. 3 shows temperatures $T_{es}$ and densities $n_{es}$ at the upstream separatrix position for quasi steady-state NBI discharges (SDC, $P_{NBI}^{abs} = 1.4$ MW) and compares downstream peak temperatures $T_{ed}$ and densities $n_{ed}$ at

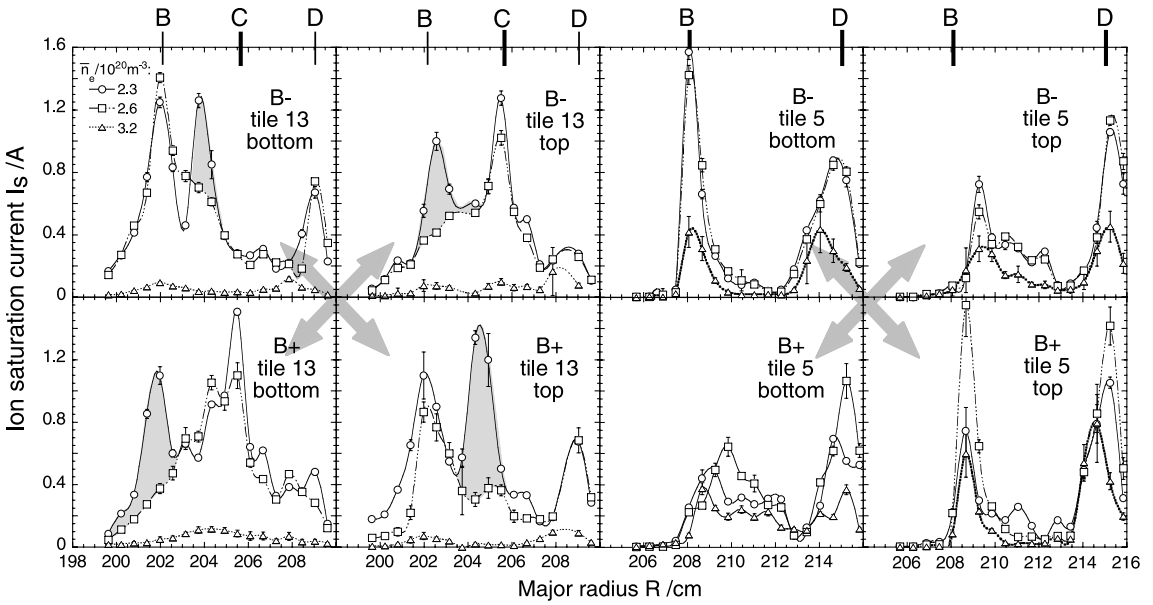


Fig. 2. Ion saturation current poloidal profiles measured by probe arrays at target tiles 5 and 13 (top and bottom) in NBI discharges ($P_{\mathrm{NBI}}^{\mathrm{abs}} = 1.4$ MW) at negative (B−) and positive (B+) magnetic field direction. Letters and short lines at the top indicate island fan positions corresponding to Fig. 1(a). Thin lines indicate positions which should be mutually shadowed by other target modules. Gray shaded areas and arrows elucidate a top/bottom asymmetry which inverts with field reversal.

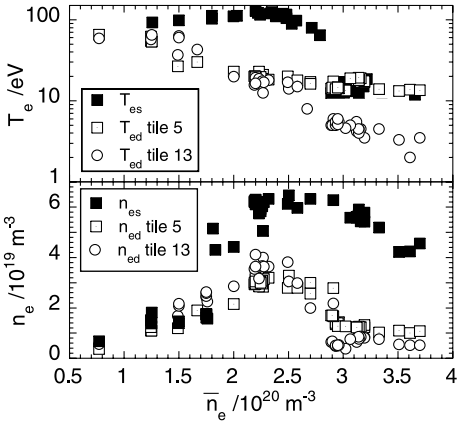


Fig. 3. Electron temperature $T_{\mathrm{es}}$ at the upstream separatrix position, peak temperatures $T_{\mathrm{ed}}$ measured by probe arrays at bottom target tiles 5 and 13, and corresponding densities as functions of the line-averaged density $\bar{n}_e$ for NBI discharges (SDC, $P_{\mathrm{NBI}}^{\mathrm{abs}} = 1.4$ MW). $T_{\mathrm{ed}}$ at tile 13 indicates detachment above $\bar{n}_e \approx 3 \times 10^{20}$ m$^{-3}$, whereas $T_{\mathrm{ed}}$ at tile 5 stays above 10 eV.

tiles 5 and 13 (bottom target) as functions of $\bar{n}_e$. At $\bar{n}_e \approx 2.5 \times 10^{20}$ m$^{-3}$, the upstream parameters start to decrease, $T_{\mathrm{es}}$ due to increasing radiation from inside the separatrix and decreasing net power flux across the separatrix, and $n_{\mathrm{es}}$ probably due to more inward shifted refueling sources. Concomittant with this, the $n_{\mathrm{ed}}$ values show rollover. At $\bar{n}_e \geqslant 3 \times 10^{20}$ m$^{-3}$, $I_s$ at tile 13 is reduced to nearly zero (see the example at $\bar{n}_e = 3.2 \times 10^{20}$ m$^{-3}$, Fig. 2), and $T_{\mathrm{ed}}$ decreases to about 5 eV or even less ($H_\alpha/H_\gamma$ intensity ratio <30 [6]) indicating detachment, whereas $T_{\mathrm{ed}}$ at tile 5 stays above 10 eV even at the highest density. This local inhomogeneity is what we define as 'partial detachment'. An inside/outside asymmetry of the upstream separatrix temperature $T_{\mathrm{es}}$ – finally caused by specific properties of the configuration – is assumed to be responsible for this feature. The low $T_{\mathrm{es}}$ values at detachment shown in Fig. 3 are incompatible with attachment on tiles 1–6. They were measured by Thomson scattering at the radial inside (mid plane) of a triangular cross-section (Fig. 1 in Ref. [1]). Flux tubes from this range end at the target region where detachment occurs, whereas tubes ending at tiles with low numbers have closest contact to the main plasma at the outside of elliptic cross-sections. Flux surfaces and islands are radially strongly compressed in this latter regions, thus favouring cross field transport and reducing the volume for efficient radiative losses from the SOL. Both effects should lead to higher upstream temperatures in this ranges and, hence, to an increased power flux onto the corresponding target region. There is not yet experimental evidence for such an asymmetry of $T_{\mathrm{es}}$, but EMC3–EIRENE code simulations support this assumption. As a first approach, the carbon concentration was assumed to be constant at 1.2%; the net power flowing across the separatrix and the upstream density were adapted to experimental conditions. The results

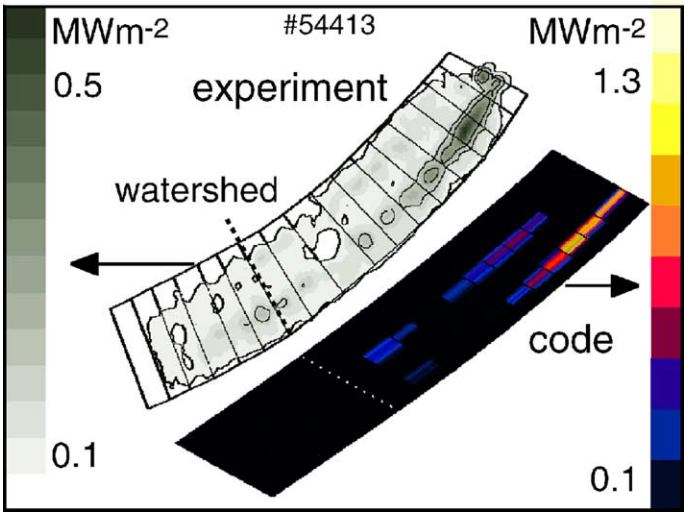


Fig. 4. Power deposition patterns from thermography for a partially detached NBI discharge (SDC, $P_{\mathrm{NBI}}^{\mathrm{abs}} = 1.4$ MW, $\bar{n}_{\mathrm{e}} = 3.5 \times 10^{20}$ $\mathrm{m}^{-3}$) and simulation by the EMC3–EIRENE code. Differences in the absolute values could at least partially be due to the neglection of impurity transport in the simulation (see text).

satisfactorily reproduce respective power deposition patterns from thermography as is shown in Fig. 4 for a case with partial detachment. Corresponding $T_{\mathrm{es}}$ values for that case show the expected asymmetry, 15 eV at the radial inside and 30 eV at the outside. In the experiments, partially detached scenarios with edge radiated power fractions of up to about 90% and a reduction of the peak thermal load even on target tiles 1–6 by up to factors 5–6 could be quasi steadily maintained [1–4], whereas complete detachment was only transiently observed in thermally unstable discharges close to the density limit.

An overview of the existence range of stable partial detachment together with that of the HDH regime in the

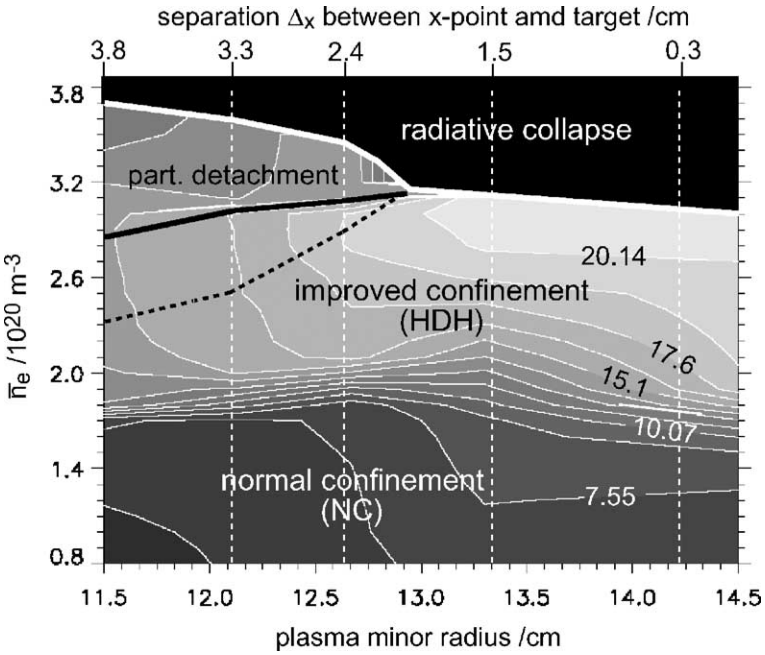


Fig. 5. Contours of the energy confinement time $\tau_E$ for NBI discharges ($P_{\mathrm{NBI}}^{\mathrm{abs}} = 1.4$ MW) indicating the existence range of the HDH regime and stable, partial detachment in the configurational space studied so far. The dotted and solid black lines indicate rollover of the particle flux onto target region 7–17 and the transition to partial detachment, respectively.

configurational space studied so far is depicted in Fig. 5. Plotted are $\tau_E$ contours for NBI heated ($P_{\mathrm{NBI}}^{\mathrm{abs}} = 1.4$ MW) discharges as functions of the line-averaged density $\bar{n}_e$ and the plasma minor radius $a$ – varied by control coil currents – for separatrix-bounded configurations with $\iota_a \approx 5/9$. Increasing plasma minor radii correspond to decreasing minimum separations $\Delta_x$ between $x$-points and targets (see Fig. 1(a)) and to decreasing radial widths of the magnetic islands. With the exception of the shortest $\Delta_x$ case, $L_c$ (taken at 1 cm inside the SOL) has been kept approximately constant at about 100 m (about 30 m from near the $x$-points to the targets). The figure shows that partial detachment is restricted to divertor configurations with $\Delta_x > 2$ cm. Otherwise the targets act as limiters. In configurations with maximum $\Delta_x$ but significantly increased $L_c$ (decreased field line pitch, reduced role of parallel relative to cross field transport), a limiter like behaviour without stable detachment was observed. Partial detachment extends the radiative density limit towards higher values without strong degradation of $\tau_E$. During partial detachment, the downstream parameters $n_{ed}$ and $T_{ed}$ are, within the error limits, close to those shown in Fig. 3 and do not significantly change with the configuration. Rollover of the ion saturation currents (particle fluxes) as well as the transition to partial detachment shift with decreasing $\Delta_x$ towards higher density.

## 5. Summary and conclusions

The new island divertor in W7-AS has substantially extended the operational range. It enables quasi steady state operation with NBI at very high density, including regimes with stable partial detachment from the divertor targets. The interaction zones on the targets show, however, a multifarious picture which deviates in many respects from distributions expected from the vacuum field geometry. Experiments with reversed $B$-field as well as first code simulations give strong indication that they are affected in first order by $E \times B$ drifts. This is expected to be of general importance for island divertors, and corresponding edge codes have to include such effects in order to allow data interpretation as well as reliable predictions. Detachment is always partial in W7-AS. At certain small target regions the plasma stays generally attached, which is probably caused by an in/out temperature asymmetry at the separatrix. Stable partial detachment is restricted to divertor configurations with sufficiently large separation $\Delta_x$ between $x$-points and targets and not too small ratios $\Delta_x/L_c$. Partially detached scenarios could be quasi steadily maintained with edge radiated power fractions of up to about 90% and a reduction of the peak thermal load even on attached regions by up to factors 5–6.

## References

[1] P. Grigull et al., Plasma Phys. Control. Fusion 43 (2001) A175.
[2] P. Grigull et al., Proceedings of the 12th International Toki Conference on Plasma Physics and Control, Nuclear Fusion (ITC12), Toki, Japan, 2001, J. Plasma Fusion Res. Series, in press.
[3] K. McCormick et al., PRL 89 (2002) 015001.
[4] K. McCormick et al., these Proceedings.
[5] Y. Feng et al., these Proceedings.
[6] U. Wenzel et al., these Proceedings.